17th Australasian Fluid Mechanics Conference
Auckland, New Zealand
5-9 December 2010

Effect of initial conditions on flow past grids of finite extension

F. Pierella[1], L.R. Sætran[1]

[1]Norwegian University of Science and Technology,
Faculty of Engineering Science and Technology, N-7491 Trondheim,

Abstract

The flow behind two circular grids of equal diameter but different mesh geometry was investigated via PIV measurements, CFD simulations and wind tunnel flow visualizations, at $Re_D = 8 \cdot 10^4$. It was found out that the grid made of biplane mesh induced a non-axisymmetric flow characterized by double-peaked non-dimensional velocity profiles, and that the wake mean flow was dominated by trailing vortices originating on the edges of the disc. These eddies create an imbalance in the entrainment of fluid from the free flow and induce the wake unevenness. The grid made of monoplane mesh instead created an axisymmetric wake, whose non-dimensional shape is described by a Gaussian interpolant, and well agrees with the literature. The downstream bars of the biplane mesh disc give birth to a known type of flow instability: their wakes interact with each other, bend radially and originate a wide recirculation area right downstream from the centre of the disc. The C_D of the biplane disc resulted to be 10% lower than the C_D of the monoplane one.

Notation

Symbol	Description
L	Mesh element side length
D	Porous disc diameter
R	Porous disc radius
σ	Disc porosity [Open frontal area / Total frontal area]
Wi	Wind tunnel/ Simulation domain width
He	Wind tunnel/ Simulation domain height
Le	Wind tunnel/Simulation domain length
I	Turbulence Intensity
Re_X	Reynolds number based on parameter X
M	Mesh size
U_0	Centreline velocity deficit
U_∞	Freestream velocity
U^*	Non-dimensional velocity
G	Spatial density of measurements
Gh	Sampling grid, horizontal size
Gv	Sampling grid, vertical size
U, V, W	Mean velocity components

Introduction

Grids and meshes are utilized in fluid flows in order to create a pressure drop thereby smoothening and attenuating the velocity profiles and to break up and homogenize the turbulence structure.

Grids of an overall axisymmetric shape — also called porous discs — mostly induce an axisymmetric wake. They were successfully employed as static wind turbines simulators in wind tunnel studies [1].

The far velocity field of axisymmetric wakes — ranging from 10D downstream on — was carefully studied and modelled in many works [4],[6], highlighting the great importance of initial conditions with respect to far wake development. Not much literature regarding near wake studies of porous discs exists; much more information is instead available about the interaction of squared and circular slender cylinders in various reciprocal arrangements, like parallel, staggered, and perpendicular.

For example, Fox [2] investigated the flow around two cylinders of square cross -section arranged perpendicular to each other, in a steady, low-turbulence, uniform flow at $\mathrm{Re_L} = 1 \cdot 10^4$, $\mathrm{Re_L} = 2 \cdot 10^4$. Complex three-dimensional interference effects were found to exist in the wake of the cylinders, whose structure was found to be strongly dependent upon their spacing. If the distance between the axes of each cylinder is less than three diameters, the interference effects are dominated by secondary flows associated with horseshoe vortex structures generated at the centre of the configuration. Kim [5] and Guillaume [3] have researched on the interaction of arrays of parallel cylinders, observing the occurrence of stable, unstable, and quasi-stable flow regimes at various cylinders distance.

This report is focused on the near wake characterization of two porous discs made up of a coarse mesh. The two discs had the same circular overall shape, porosity and mesh element size, where the porosity σ is defined as solid frontal area over total frontal area. In facts, both grids were made up of two perpendicular arrays of regularly spaced squared cylinders, but while in the monoplane grid the axes of the cylinders intersected; in the biplane grid they had an x-wise spacing of L (figure 1). The mesh is squared and not axisymmetric for ease of construction; the size L of the mesh elements is comparable to the mean chord length of the blades of a wind turbine model used for former wake interaction experiments.

Despite the fact that both discs had the same circular shape, the biplane disc generated a non-axisymmetric wake, while the monoplane disc developed an axisymmetric wake. The main purpose of this paper is thus to address the following issue: why does this happen? What factors influence the wake development? As an investigation tool, the shape of the non-dimensional velocity profiles U^* with respect to downstream distance was analysed. Particular attention was devoted in addressing the presence of coherent structures in the wake velocity field.

The analysis consisted of both measurements and computer simulations. Velocity measurements were performed via PIV and via a Pitot tube in the near wake region (zero to 6D downstream from the disc). Support to experimental hypotheses was looked for in flow visualizations by means of smoke and tuft wires. The results of the experiments were extended and refined through Fluent® CFD simulations.

Experimental Arrangement

Measurements and simulations were carried out with different experimental configuration. Each subsection deals with the description of one experimental arrangement.

PIV measurements

PIV tests were performed at $Re_D = 8 \cdot 10^4$, in a closed loop wind tunnel, both on a biplane and on a monoplane disc. The free stream velocity was monitored via a Pitot tube positioned 5D

upstream from the disc, and it has proven to be constant during the test within a ±1% uncertainty.

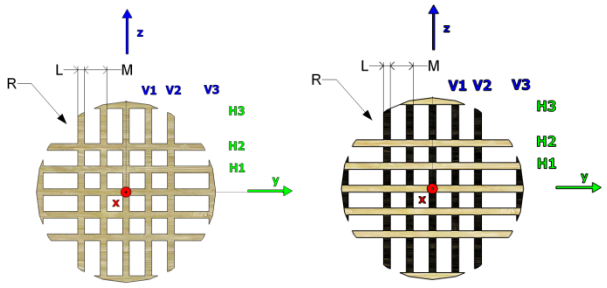

Figure 1. The porous discs, monoplane (a) and biplane (b), seen from downstream. In (b), the x-wise distance between the axes of the arrays of bars is L. We report also the nomenclature convention used for the bars: H stands for horizontal, V for vertical. The x^+ axis is directed outward from the page.

Experimental Parameters				
Test	**PIV**	**Pitot**	**Sim**	**Smoke T**
L [cm]	0.3	1	3	0.3
M [cm]	1	3.3	10	1
D [cm]	8	80	80	26.6
Re_D	$8{\cdot}10^4$	$8{\cdot}10^4$	$8{\cdot}10^4$	$2.7{\cdot}10^4$
Wi×He [m]	1×0.5	1.8×2.5	1.6×1.6	Open
I [%]	1	1	1	-
Tested Grids (Bi- or Monoplane)	B/M	B	B/M	B

Table 1. Summary of some geometrical parameters

The air temperature variations were monitored and were considered negligible for the current tests. The tunnel dimensional characteristics are reported in table 1. The solid and wake blockage factor of the wind tunnel due to the disc presence were considered negligible.

The PIV system was a commercial 2-D DC-PIV system from Dantec Dynamics, of the double-frame double-exposure type. The main components are listed in table 2. The wind tunnel was equipped with two optical accesses for the camera and the laser: the resolution of the camera (1600×1196 pixels) and the dimension of the smoke tracing particles (around 10 µm) limited the field of view for a single camera picture to 100×75 mm. Flow Manager® software, from Dantec Dynamics, was used to compute instantaneous velocity field computation. The choice of a 32×32 pixels interrogation window allowed to compute 100×73 vectors each couple of acquired pictures. Subsequently, mean velocity fields were calculated as the average of 110 instantaneous velocity fields, via the same software mentioned before.

To reconstruct the mean disc wake up to 8D downstream we needed to assemble together several mean velocity fields, and therefore to measure multiple side-to-side positions. Practical considerations showed it was more convenient to move the disc instead of the whole PIV system: the disc was thus installed on a two-direction manual traversing system. A Matlab® routine was elaborated to assemble together the several mean velocity fields.

In figure 2 a sketch schematizes the experimental setup.

PIV		
Item	**Characteristics**	**Note**
Camera	FlowSense 2M 10bit	-
Smoke Generator	Safex Fog Generator FOG 2005	-
Laser	New Wave Solo PIV II	Nd-Yag laser

Table 2. PIV instrumentation

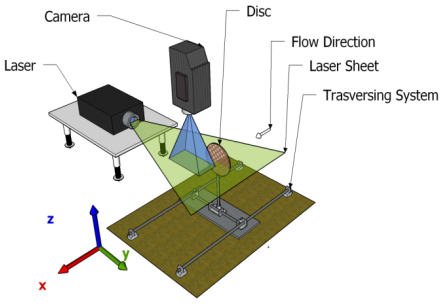

Figure 2. PIV setup. For the biplane grid, the downstream bars are oriented along the y.-axis.

Pitot tube measurements

Far wake Pitot tube measurements were performed in a closed loop wind tunnel at $Re_D = 8 \cdot 10^4$. Only the biplane grid was tested. The dimensional and free flow turbulent characteristics are summarized in table 1. The free stream velocity was monitored through a Pitot tube positioned on the inlet of the test section; the free stream velocity varied within ±1% during the test campaign. The temperature variations were monitored and appropriate corrections to air density were applied. The wake was traversed at several downstream distances by means of a 3D traversing system with a positional accuracy of ±1 mm. The Pitot tube pressure output was routed to a differential pressure transducer, and hence 1000 samples for each sampling position were acquired via a NI USB data acquisition device, and then saved and elaborated through Labview® software. As it can be seen on figure 3, the wake was sampled on the yz plane, while the free stream velocity U_∞ is directed on the x axis. The spatial density has the value of $G = 3\,cm$. The horizontal and vertical size of the sampling grid were adapted from time to time as the size of the wake increased with increasing downstream distance, while the spatial density of the points has been kept constant.

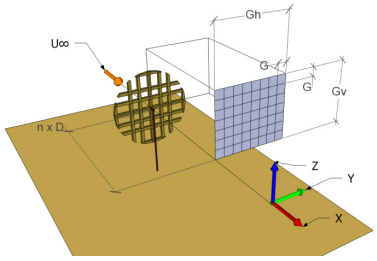

Figure 3. Pitot measurements setup. G is the measurement spatial density; U∞ the free stream velocity, n × D the varying downstream distance. Downstream bars are oriented along y-axis for the biplane grid.

Simulations

To extend the experiment data, near-wake CFD studies have been carried out. Simulations were performed by means of Ansys Fluent® software package, on both monoplane and biplane grids. To be consistent with the measurements, a $Re_D = 8 \cdot 10^4$ was achieved. A free stream turbulence intensity of 1% was set. The method chosen was a 7-equation RANS, which appeared to be a good compromise between precision and computational effort. The Reynolds stress model was set to linear pressure-strain; standard wall functions were employed. Only one quarter of disc was modelled and meshed, for symmetry reasons. The analysis volume measured 6.4×1.6×1.6 m, and the disc was shaped with the dimensions of a former bigger disc model, that is to say $L = 3\,cm$, $M = 10\,cm$, $D = 80cm$. The computational mesh is of tetrahedral type, with a maximum face and tetrahedron size of 4 cm. The total number of nodes was 3.67 million, and the mesh has been refined in the proximity of the disc to achieve a greater precision in the critical zone in-between the bars.

Disc construction

As it can be deduces from table 1, four discs of different dimensions were constructed, two with biplane and two with monoplane grid, with D = 8 and 26.6 cm. All of them were made of common pine wood. The arrangement of the bars and a clear insight into the meshes type difference can be found in figure 1. The porosity relative to the whole disc is $\sigma = 55\%$.

Parameters estimation

The velocity profiles were non-dimensionalized with the following conventions, used and reported by [6]. U* was calculated as follows:

$$U^* = \frac{U_\infty - U}{U_0} \quad (1)$$

$$U_0 = U_\infty - U_{CL} \quad (2)$$

$$U_{CL} = U(x_0, 0, 0) \quad (3)$$

where U_{CL} is the x-component of the U velocity at the centre of the wake at x_0 downstream distance, and U_0 is the difference between this quantity and the free stream velocity.

The non-dimensional drag force on the disc was calculated as follows:

$$C_D = \frac{D}{{}^1/_2 \rho U_\infty^2 A} \quad (4)$$

Where D is the total drag force, ρ is the density of the air, U_∞ is the free stream x-component of the velocity vector, and $A = \pi R^2$ is the total frontal area of the disc.

Experimental Results

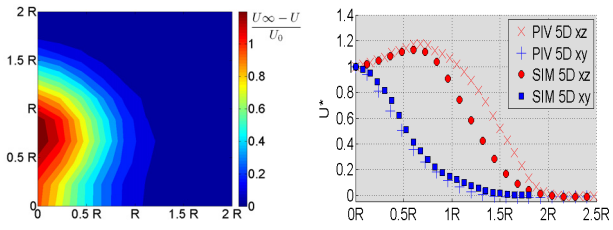

Figure 4. (a) Wake at 5D downstream, biplane grid, yz-plane, Pitot tube measurements. (b) xz and xy 1D normalized velocity profiles, PIV measurements vs. Simulations.

Pitot tube measurements at different downstream distances from the disc revealed a profoundly different flow pattern between the monoplane and the biplane discs wake. At 5D (figure 4), the biplane disc wake on plane zy is non-axisymmetric, despite the axisymmetric shape of the wake generator. The wake is broader in y-direction than z-direction, and the maximum velocity deficit is not in the x-axis, but shifted 0.5R upwards. The non-dimensional velocity profiles quantify the difference between the xy and the xz planes. The xz profile shows a peculiar peak at 0.5R, and confirms that the momentum deficit in this plane is much higher than in the xz. The monoplane wake is instead axisymmetric, and has a regular bell shape: already at 5D the non-dimensional profile can be well interpolated by a Gaussian curve, see figure 5. Comparisons with Johansson's axisymmetric wake measurements [4], confirmed a good degree of agreement between the non-dimensional shapes of the velocity profiles.

Near wake PIV measurements (0D to 6D downstream) were performed for both discs on xy and xz planes (see figure 2 for reference).

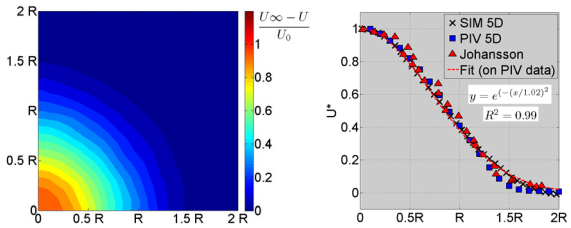

Figure 5. (a): wake at 5D downstream, monoplane grid, yz-plane, Simulation (b): comparison of normalized U data for 1D velocity profile, between simulations, PIV measurements and Johansson [4]. The fitting is referred to the simulations results. Fitting equation: $U^* = \exp\left(-\frac{x}{1.02}\right)^2, R^2 = 0.99$

Preliminary measurements proved the symmetry of the wakes on the measurement planes, which allowed us to perform measurements only on half of the wake. About 20 mean velocity fields had to be assembled to reconstruct the desired velocity field. The contour plots of the U velocity field are reported in figure 6 for the biplane and the monoplane disc.

It is clear, observing the xz_b plane —the "b" subscript stands for biplane, "m" for monoplane — how the jets originated from the spacing of the mesh join together and diverge towards the outer part of the wake, creating a wide negative velocity zone (0.5D × 0.25R). The xy_b wake features a recirculation area in correspondence of the centre of the disc, but less extended than the xz_b plane one (0.1D × 0.1R). In fact, as the measurements planes are perpendicular, the centreline profiles of velocity should be the same, and the negative velocity zones should have at least the same length. This error was imputed to an involuntary shift towards the z^+ direction of the xy_b measurement plane of about 0.1R. Simulations showed that the error on measured velocities due to such a shift falls to less than 5% already at 2D downstream.

The xz_m wake of the monoplane disc highlights a different behaviour: the grid-generated jets do not merge and persist parallel to the main flow, without the occurrence of any recirculation.

Taking a look at the xz_b flow field in figure 6a, we notice that the flow pattern created by the wakes of the squared cylinders forming the downstream mesh (or, in other words, of the grid-generated jets) is very similar to the one reported by Guillaume [3] in his experiments. At similar Reynolds, $Re_L = 2.5 \cdot 10^3$, he observed a quasi stable behaviour of the flow pattern downstream an array of 3 parallel cylinders, where the wake of the central bar was much wider than the two side bars wakes. This behaviour, though, has been reported for smaller (0.8 to 1.2) spacing ratios, defined as the ratio between the distance and the side length of the cylinders, in this work $(M - L)/L = 2.33$. This instability is a known issue for flows through array of bars and cylinders, though the reasons for its occurrence are still under investigation, as reported by [3],[5].

In figure 6b, which reports the transverse velocity component contour plots, marked upward velocity components are generated immediately downstream from bars H1 and H2, whose intensity goes up to $0.4U_\infty$. The recirculation area downstream from the centre of the disc features a wide area with downward velocity component. On the xy_b plane, a streak of negative velocity fluid originates from the bar H3, and the measurements show that it is observable up to 5D downstream.

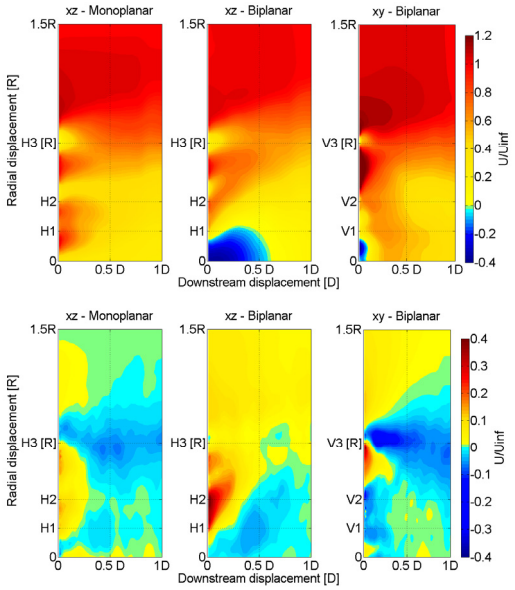

Figure 6. Longitudinal (a) and transversal (b) velocities for different sections of the disc wake, PIV measurements. Flow from left to right.

A similar behaviour was observed on the xz_m plane in correspondence of bar H3, though the negative velocity area is not as much extended, and not as intense. This negative velocity component is most likely the responsible for the strong shrinking of the wake on the xy_b plane. The mechanisms which create the flow non-homogeneity are not evident from what we have said so far. Better clues arise from the investigation of the yz vector field of the monoplane and biplane wakes, reported in figure 7 and 8.

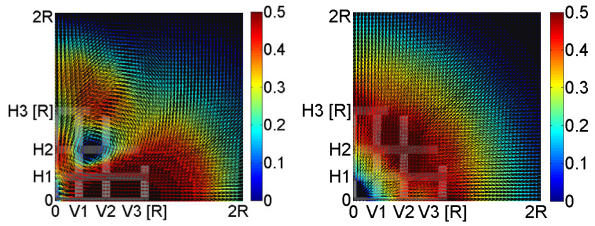

Figure 7. Transverse velocity field at 5D downstream, yz-plane. (a) Biplane grid, (b) Monoplane grid. Units are in $\sqrt{(V+W)^2}/U_\infty$. The flow is directed outwards from the page.

At 0.5D downstream (figure 8b), simulations showed that two dominant vortices originate from the tips of bars H3 and H2, and both vortices spin in the same clockwise direction. The vortices extend downstream in the same fashion of a trailing edge vortex created by the tip of a wing. At 5D downstream, the two trailing vortices have already merged, and only one big vortex is visible, approximately centred on the crossing between bar H2 and V2 (see figure 7a). The vortex entrains fresh fluid from the free stream along the y direction and drags it into the wake; for this reason, the y-width of the wake is lower than the z-width. One can also see how the tangential velocity of the vortex is higher in the y direction than in the z direction: more fluid is entrained in the wake than is dragged out by the vortex itself. This may explain the non-axisymmetry of the wake and the formation of central peak in the xz_m plane wake velocity profile. The trailing vortex occurring on the tip of bar 3V, highlighted by the simulations, has been confirmed by flow visualizations performed via tufts, see figure 8a. As a further element, no vortices appear in the monoplane yz wake (figure 7b).

Horseshoe trailing vortices generated by two cylinders in cross arrangement have been observed by Fox [3] ad Zdravkhovich [7]. With the presence of the vortices, a drag reduction of the cross layout with respect to single cylinders was observed.

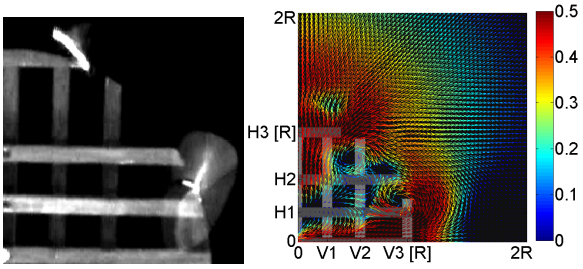

Figure 8. (a)Vortex originating on bar V3, visualized via tuft wires. Superimposition of 10 camera frames, at ReD=8·10³. (b) yz-plane velocity field at 0.5D downstream, from Simulations.

The flow object of this work is much more complex flow than the one in Fox's work, and we still do not have enough evidences to state whether the mechanisms producing the observed trailing vortices is the same responsible for the horseshoe vortices there reported. It is a matter of fact, anyway, that such trailing vortices have not been observed in the monoplane grid arrangement (see figure 8b), and that the biplane grid drag resulting from the simulations is $C_{D,b} = 0.73$ — 9% lower than the corresponding biplane grid drag, $C_{D,m} = 0.79$.

Conclusions

The flow pattern downstream from two porous meshes has been studied via PIV and Pitot tube measurements, CFD simulations and wind tunnel flow visualizations, at a $Re_D = 8 \cdot 10^4$. It was found that the biplane grid induces a non-axisymmetric wake dominated by the presence of trailing vortices. These vortices entrain fresh fluid from the surroundings in a non-symmetric fashion, and are the responsible for the wake unevenness and the two-peaked shape of the velocity profiles. The downstream array of cylinders induces a flow pattern observed before by Guillaume [3], where the wakes of the cylinders interact with each other in a quasi-stable way. The role of this flow pattern on the wake development has to be further investigated. The monoplane disc induces an axisymmetric wake, whose non-dimensional shape is well described by a Gaussian curve. The biplane disc is characterized by a drag coefficient 10% lower than the corresponding monoplane one, which is in agreement with the observations reported by Fox [2].

References

[1] S. Aubrun, "Modelling wind turbine wakes with a porosity concept," *Journal of Wind Engineering and Industrial Aerodynamics,* 2005, pp. 265-270.

[2] T. Fox, "Interference in the wake of two square-section cylinders arranged perpendicular to each other," *Journal of Wind Engineering and Industrial Aerodynamics*, vol. 40, pp. 75-92, 1992.

[3] D. Guillaume and J. LaRue, "Investigation of the flopping regime with two-, three-and four-cylinder arrays," *Experiments in Fluids*, vol. 27, pp. 145-156, 1999.

[4] P. Johansson, "The axisymmetric turbulent wake," *Doctoral Thesis*, Chalmers University of Technology, vol. 1860, 2002.

[5] H. Kim, "Investigation of the flow between a pair of circular cylinders in the flopping regime," *Journal of Fluid Mechanics*, vol. 196, pp. 431-448, 2006.

[6] P. Kundu and I. Cohen, "Fluid Mechanics. 2004," ed: Elsevier Academic Press.

[7] M. Zdravkovich, "Interference between two circular cylinders forming a cross," *Journal of Fluid Mechanics*, vol. 128, pp. 231-246, 2006